# SLOW CONDUCTION IN CARDIAC MUSCLE

## A Biophysical Model

MELVYN LIEBERMAN, J. MAILEN KOOTSEY,
EDWARD A. JOHNSON, *and* TOHRU SAWANOBORI
*From the Department of Physiology, Duke University Medical Center, Durham, North Carolina 27710*

ABSTRACT Mechanisms of slow conduction in cardiac muscle are categorized and the most likely identified. Propagating action potentials were obtained experimentally from a synthetically grown strand of cardiac muscle (around 50 $\mu$m by 30 mm) and theoretically from a one-dimensional cable model that incorporated varying axial resistance and membrane properties along its length. Action potentials propagated at about 0.3 m/s, but in some synthetic strands there were regions (approximately 100 $\mu$m in length) where the velocity decreased to 0.002 m/s. The electrophysiological behavior associated with this slow conduction was similar to that associated with slow conduction in naturally occurring cardiac muscle (notches, Wenckebach phenomena, and block). Theoretically, reasonable changes in specific membrane capacitance, membrane activity, and various changes in geometry were insufficient to account for the observed slow conduction velocities. Conduction velocities as low as 0.009 m/s, however, could be obtained by increasing the resistance ($r_i$) of connections between the cells in the cable; velocities as low as 0.0005 m/s could be obtained by a further increase in $r_i$ made possible by a reduction in membrane activity by one-fourth, which in itself decreased conduction velocity by only a factor of 1/1.4. As a result of these findings, several of the mechanisms that have been postulated, previously, are shown to be incapable of accounting for delays such as those which occur in the synthetic strand as well as in the atrioventricular (VA) node.

### INTRODUCTION

Slow conduction in heart muscle (apparent velocity $<0.1$ m/s) is best exemplified in the region of the AV node (1, 2). Slow conduction has also been observed in isolated Purkinje fibers (3), branches of the His bundle (4), and between Purkinje fibers and ventricular muscle cells (5, 6). Slow conduction is also a necessary requirement for the phenomenon of reentry, the mechanism postulated for the genesis of arrhythmias in cardiac muscle (3).

Several mechanisms have been postulated to account for slow conduction. These hypotheses fall into three general categories: (*a*) variations in geometry (7–11), and

changes in (*b*) membrane properties (3, 7, 10, 12, 13) and (*c*) intercellular connections (9, 10, 14–16). The present paper exploits the relatively simple geometry of a synthetically grown strand that was designed to avoid the electrophysiological complications of a two- or three-dimensional syncytial structure and the mechanical difficulties of the thick collagenous matrix and the enveloping endocardial sheath of its naturally occurring counterpart (17). The synthetic strand is realistically modeled as a one-dimensional cable and the number of parameters and thus the ways of slowing propagation are restricted.[1]

## METHODS

### *The Preparation*

The methods for growing isolated heart cells in linear arrays (strands) have been described in detail elsewhere (17). In brief, the tissue culture procedure was as follows. Hearts were dissected aseptically from chick embryos incubated 11–13 days, minced in saline G at 37°C, and disaggregated in 0.1% trypsin-saline G for 10 min. The trypsinization was stopped by adding cold culture medium and the cell suspension was then filtered, centrifuged at 1200 rpm for 5 min, and after removal of the supernatant, the remaining pellet was resuspended in culture media. Cells were plated at known densities ($10^5$–$10^6$ cells per culture dish) on a differentially treated surface consisting of an agar gel containing channels of exposed collagen approximately 25 $\mu$m wide. The cultures were incubated at 37°C in a humidified chamber containing 5% $CO_2$/95% air. The culture media contained Eagle's minimum essential medium (MEM) or medium 199 supplemented with 10% fetal calf serum, 2% chick embryo extract, and a 1% mixture of penicillin G and streptomycin sulfate.

During the electrophysiological observations, the surface of the culture medium was covered by a layer of nontoxic mineral oil (Klearol, Witco Chemical Co., Inc., New York) to prevent evaporation of the culture medium (18). The culture dish was placed on an inverted phase microscope (model M, Nikon, Inc., Div. of EPOI, Garden City, N. Y.), the stage of which was maintained at 37°C by dissipating regulated DC power in two power resistors (Dale Electronics Inc., Columbus, Neb., RH-10) bolted on opposite sides of the stage. The pH was kept constant by streaming a warmed mixture of air and $CO_2$ over the surface of the mineral oil.

The preparation was stimulated extracellularly through a bevel-edged, glass microelectrode (50 $\mu$m tip diameter) (19) filled with 0.5% agar/saline G and connected via a saline G bridge/silver wire to the output of a stimulus isolation unit (model ISA 100, Bioelectric Instruments Div. of General Microwave Corp., Berkeley, Calif.) driven by a pulse generator (160 series, Tektronix, Inc., Beaverton, Ore.). This stimulating electrode was attached to a miniature micromanipulator (model HS, Brinkmann, Brinkmann Instruments, Inc., Westbury, N. Y., coupled with a micrometer-head drive, Lansing Research Corp., Ithaca, N. Y.) mounted on the stage of the microscope. With this arrangement, the stimulating electrode moved with the stage and remained fixed with reference to the preparation. Transmembrane potentials were recorded with glass microelectrodes filled with 3 M KCl; the electrodes had a resistance which ranged between 40–60 MΩ. A silver wire connected the microelectrode to a

[1] Preliminary reports of portions of this work were given at the meeting of the Federation of American Societies for Experimental Biology (Lieberman, Kootsey, Johnson, Roggeveen, 1971), and at the annual meeting of the Society of General Physiologists (Lieberman, Purdy, Roggeveen, Johnson, 1971).

guarded input probe amplifier (20). Two peripherally placed silver wires formed return and reference electrodes; rectangular voltage calibrating pulses (model CA5, Bioelectric Instruments Div. of General Microwave Corp.) were applied between the reference electrode and ground. The output of the amplifier was displayed on a dual beam oscilloscope (type 565, equipped with types 3A3 and 3A74 plug-in units, Tektronix, Inc.) and photographed with an oscillographic camera (model C4, Grass Instrument Co., Quincy, Mass.). Conduction velocities were calculated from measurements of the activation time to each recording site (considered as the time between the stimulus artifact and a point at 50% of the total upstroke amplitude) and the distance between either two recording electrodes or one recording electrode and the stimulating electrode. Composite photomicrographs of the relative positions of each electrode were made either directly through the microscope with a Polaroid Land camera (Polaroid Corp., Cambridge, Mass.) or from the monitor of the television system (see below) with a 35 mm camera equipped with a Polaroid back (Nikon F with Speed Magny, Nikon, Inc., Div. of EPOI).

Small preparations of cardiac muscle (21), and particularly the synthetic preparation of the kind used here, offer a number of advantages over other preparations of cardiac muscle: they have a relatively simple geometry and microelectrodes can be positioned with respect to each other and inserted under direct microscopic control. We found intracellular recordings from such preparations difficult. There appeared to be two main problems. One, mechanical vibration of the electrode with respect to the tissue and secondly, the need to provide a sudden, but controlled stabbing motion to the electrode for final impalement. We have overcome each of these difficulties in the following manner. Cell impalements were watched with a high power, enhanced contrast, television microscopy system (21) with an effective magnification up to 230 $\mu$m per horizontal line. The electrodes were positioned at the surface of the strand by Leitz micromanipulators (E. Leitz Inc., Rockleigh, N. Y.). Final impalement of the cell was made by momentarily vibrating the electrode along its longitudinal axis. Each electrode was strapped to a piece of balsa wood cemented to the center of a cone of a 1½ inch diameter loudspeaker (model TS 19, Philmore Mfg. Co., Inc., Richmond Hill, N. Y.) and driven by a short tone burst from an audio oscillator, the frequency of which was adjusted to select a predominantly axial mode of electrode movement (200 Hz). The television microscopy system and input amplifiers were mounted on an air-suspension, antivibration table (Barry Controls, Div. of Barry-Wright Corp., Watertown, Mass.), with isolation comparable with a 12 dB per octave low-pass filter with a 3 dB frequency cut-off at 3Hz.

### *The Model*

The synthetic strand contains columns of elongate cells, the membranes of which frequently become closely apposed, both side to side and end to end (22).[2] These regions of close cell apposition appear to be the site of resistive connection between cells, so that the tissue behaves electrically as a syncytium. For our theoretical model, we chose, as a first approximation, a single one-dimensional cable described by a modified cable equation in which the axial resistance and membrane properties could be made to vary continuously along the length of the cable. This model represents either a single column of cells or a bundle of identical columns. For the case of a bundle, variations in the number of columns along the length were simulated by making correlated variations in axial resistance and membrane area along the length.

[2] A detailed morphological description of the preparation now appears in an article by Purdy et al., 1972, *J. Cell Biol.* **55**:563.

Assuming resistance to current in extracellular space is zero, the classical one-dimensional cable equation (23) is

$$\frac{1}{r_i}\frac{\partial^2 V_m}{\partial x^2} = i_m = c_m\frac{\partial V_m}{\partial t} + i_i, \tag{1}$$

where $V_m$, the inside potential measured with respect to the outside potential (zero everywhere) varies with time $t$ and distance $x$ along the cable axis. $i_m$ is the membrane current per unit length made up of the ionic current $i_i$ and the current through a capacitance $c_m$ per unit length. $r_i$ is the resistance of the cytoplasm per unit length and is assumed in this equation to be constant; however, for our purpose we wish $r_i$ to vary along the length of the column in which case another term appears in the derivation (see Appendix) and Eq. 1 is replaced by

$$\frac{1}{r_i(x)}\frac{\partial^2 V_m}{\partial x^2} - \frac{1}{[r_i(x)]^2}\frac{\partial r_i(x)}{\partial x}\frac{\partial V_m}{\partial x} = c_m\frac{\partial V_m}{\partial t} + i_i. \tag{2}$$

A convenient form for $r_i(x)$ which will allow us to simulate a change in $r_i$ alone along the length of the cell column as well as a change in the number of columns in a bundle is

$$r_i(x) = \frac{\phi(x)}{\eta(x)}\cdot\frac{4R_i}{\pi d^2}, \tag{3}$$

where $R_i$ is the volume resistivity of the cytoplasm and $d$ is the cell diameter. The dimensionless factor $\phi(x)$ is used to vary $r_i$ alone along the length of the cell column. The dimensionless factor $\eta(x)$, proportional to the number of columns, is used to describe a change in the number of columns in a bundle in which case $\eta(x)$ must also be used to scale the membrane current per unit length (right-hand side of Eq. 2). Substituting in the expression for $r_i(x)$ and scaling the right-hand side of Eq. 2, it becomes

$$\frac{\partial^2 V_m}{\partial x^2} - \left[\frac{1}{\phi}\frac{\partial \phi}{\partial x} - \frac{1}{\eta}\frac{\partial \eta}{\partial x}\right]\frac{\partial V_m}{\partial x} = \frac{4R_i C_m}{d}\phi\frac{\partial V_m}{\partial t} + \frac{4R_i}{d}\phi I_i, \tag{4}$$

where $C_m$ is the specific membrane capacitance (microfarads per square centimeter) and $I_i$ is the membrane ionic current through a unit area of membrane.

The depolarization phase of the cardiac action potential appears to be generated, to a first approximation, by a sodium-carrying mechanism similar to that described for the squid giant axon (24, 25). Mechanisms for the generation of the repolarization phase have been proposed and mathematically described (26). Experimental findings, however, have not yet revealed the true nature of this mechanism (27). Since we were, in any case, only concerned with the propagation of depolarization and we did not want to make further assumptions which would complicate the interpretation of our results, we simulated a prolonged repolarization phase by the simple maneuver of eliminating the delayed rise in potassium conductance (28, 29). This results in an action potential which fails to repolarize, the membrane potential after the spike remaining indefinitely. The spike and early part of the plateau of the resulting membrane action potential is illustrated by curve 1 in Fig. 6. In other words, the membrane ionic current $I_i$ was described by

$$I_i = g_{Na}(V - V_{Na}) + g_K(V - V_K), \tag{5}$$

where $g_{Na}$ was described by the Hodgkin-Huxley formulation ($g_{Na} = \bar{g}_{Na}m^3h$) and $g_K$ was constant.

The one-dimensional cable is thus described by Eq. 4 together with Hodgkin-Huxley equations for the ionic currents, modified as above. Solutions for this system of nonlinear equations were obtained by digital computer methods. The length of the cable was divided into 21 equal segments and the difference equation equivalent to Eq. 4 was written and solved, together with the Hodgkin-Huxley equations for $I_i$, for each of the interior points by implicit matrix methods (30, 31). To obtain boundary conditions for the solution of the cable equation, two separate equations were written for the membrane segments at each end of the cable and solutions of these equations were advanced (by the Adams-Moulton method, [31]) one time increment ahead of the cable solution. The equations for the end segments were of the form

$$I_s + i_c = \left(c_m \frac{\partial V}{\partial t} + i_i\right) \Delta x, \tag{6}$$

where $I_s$ is the stimulating current (0.1 $\mu$A for 0.1 ms at the left end, zero at the right end) and $i_c$ is the current from the neighboring segment. The range of values for the problem parameters and the increments in length $\Delta x$ and time $\Delta t$ were as follows:

cell diameter $d$ = 3–10 $\mu$m,
cytoplasmic resistivity $R_i$ = 150–320,000 $\Omega$-cm,
membrane specific capacitance $C_m$ = 2 $\mu$F/cm$^2$,
sodium equilibrium potential $V_{Na}$ = +55 mV,
potassium equilibrium potential $V_K$ = −72 mV,
maximum sodium conductance $\bar{g}_{Na}$ = 120 mmho/cm$^2$,
potassium conductance $g_K$ = 0.36 mmho/cm$^2$,
spatial increment $\Delta x$ = 0.006–0.06 mm,
time increment $\Delta t$ = 5–50 $\mu$s.

Propagation velocity of computed action potentials was "measured" by noting the difference between the times of half-maximal depolarization of two internal segments in the cable and dividing this time difference into the distance between the segments. Running time on an XDS Sigma 5 (Sigma Instruments, Inc., Braintree, Mass.) varied between 90 s and 90 min.

Two special configurations, in addition to the above general configuration, were investigated. One was the case where two patches of excitable membrane were electrically interconnected by a passive leaky cable. The other case comprised two one-dimensional cables of excitable membrane interconnected by a single resistance. In the first of these, the interconnecting cable was described by the classical cable equation (Eq. 1) with $i_i$ equal to $V_m/r_m$ with $r_m$ (the resistance of the membrane in a unit length of cable) constant. The two membrane patches were coupled to and formed the boundary conditions for the interconnecting cable and solutions to Eq. 1 were required for each of the two cable segments.

## RESULTS

### *The Preparation*

Since isolated beating heart cells do not readily adhere to the agar substratum, they selectively attach within the channels of exposed collagen (approximately 25 $\mu$m wide) either singly or as aggregates. Spontaneously beating strands of heart cells

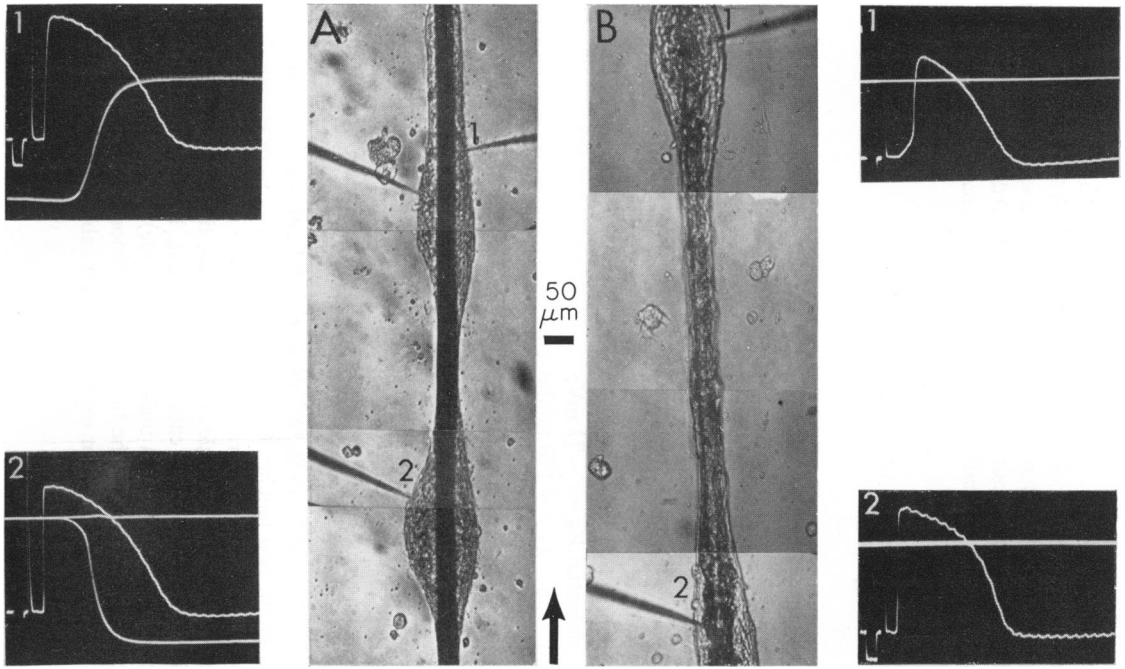


FIGURE 1 Normal (A) and delayed (B) conduction observed in synthetic strands of cardiac muscle grown in tissue culture. Arrow indicates direction of impulse propagation initiated by an extracellular stimulating electrode placed 10.8 mm (A) and 7.8 mm (B) from the lowest microelectrode (2). The lower trace in frames A 1 and A 2: upstroke of the action potential at ×25 expanded sweep (upright in A 1, inverted in A 2). Calibration pulse of 20 mV and 20 ms (normal sweep) which appears in frames A 1 and B 2 also applies to frames A 2 and B 1. × 80.

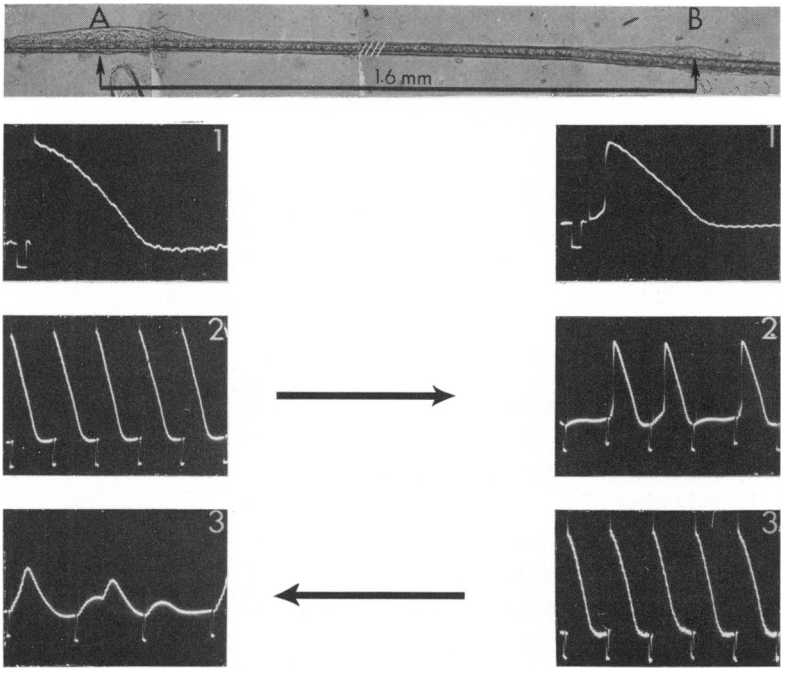


FIGURE 2 Transmembrane action potentials recorded from two bulbous regions A and B 1.6 mm apart in a synthetic strand of cardiac muscle during antegrade (1 and 2) and retrograde (3) stimulation. The apparent conduction velocity between regions A and B was 0.04 m/s. The tip of the extracellular electrode is shown adjacent to bulbous area A: it was moved to B during retrograde stimulation. The microelectrode was positioned first at A and then at B (see arrows). The hatched area (100 $\mu$m) denotes the region in which desynchronized contractions were observed at frequencies above 180 beat/min (antegrade) and 120 beat/min (retrograde). Calibration pulse: 20 mV and 20 ms. $\times$ 48.

1.0–30.0 mm in length are formed after 3–6 days in culture (17). Some strands were nearly uniform in width, ranging from 25–100 $\mu$m, whereas others had bulbous segments up to 400 $\mu$m in width tapering down to 25 $\mu$m between bulbs (Fig. 1). The structural organization of the strands consisted of an inner core of muscle cells surrounded by an outer sheath of fibroblast-like cells, i.e., the dispersed cells from the heart reaggregate and sort out with respect to cell type and spatial relationships (22).

The preparations were driven at rates (1.6–2.0 beat/s), slightly higher than the spontaneous rates. Action potentials recorded from cells in bulbous areas (Fig. 1) had either a rapid upstroke (around 100 V/s) or a noticeably slower upstroke (as low as 10 V/s) preceded by a slow prepotential. The slow rising potentials were generally lower in amplitude and of shorter duration than the fast rising potentials. In some strands, the average propagation velocity of action potentials obtained from two electrodes spaced 500–800 $\mu$m apart varied markedly from 0.02–0.8 m/s from one region to another. Tapering of the overall diameter in very short distances along a strand is not in itself responsible for the low conduction since the conduction veloc-

ity between bulbous regions in one preparation can be fast (similar to regular cardiac muscle) whereas in the other it can be slow. For example, in Fig. 1 A, the average conduction velocity in the tapered region was 0.5 m/s whereas in a similar region in Fig. 1 B it was 0.03 m/s. In a bulbous region which showed action potentials with a slow upstroke and a prepotential, the bulbous region immediately proximal to it showed normal action potentials. Other studies have shown that such interbulbous regions contain fewer cardiac muscle cells than normally propagating regions (17).

Normally, fast conducting regions followed stimulation up to about 5 beat/s and switched to 2:1 block at higher rates. In slow conducting regions not only did 2:1 block occur at slower rates (4 beat/s) but it was preceded by a cyclic progressive slowing of conduction, as illustrated in Fig. 2, each cycle being terminated by a single dropped beat (Wenckebach phenomenon). Fig. 2 B also shows that the entire region of slow conduction is between the two electrodes since action potentials recorded by the distal electrode revert to normal when the direction of excitation is reversed. Localization of the block to a 100 $\mu$m segment of this region was signaled by an interruption and reversal in the otherwise smooth motion of contraction there.

Closer electrode spacing revealed that local conduction velocities were clustered around two extreme values. For example, in Fig. 3, action potentials propagated up to the region of observed conduction failure at a velocity of 0.3 m/s (maximum for this preparation); in the slow conducting region, the velocity fell to a value of 0.002 m/s, a value comparable with the conduction velocity reported for regions within the AV ring of the embryonic chick heart (32). Action potentials recorded in this region of slow conduction were typically diminished in amplitude and with slowly rising upstrokes. The average conduction velocity in the 900 $\mu$m interbulbous

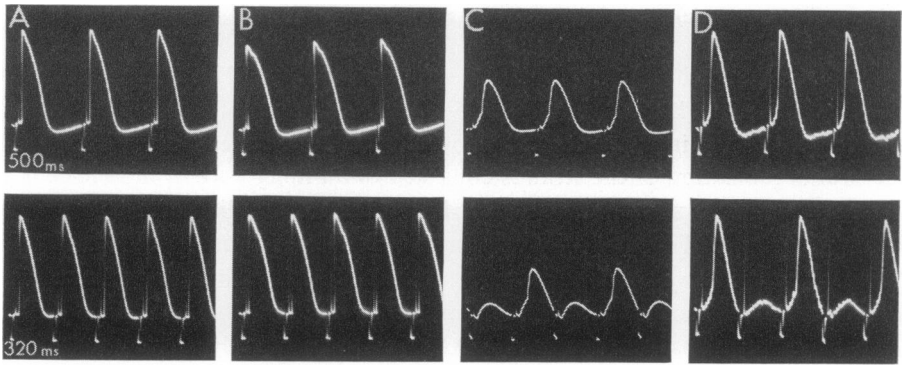


FIGURE 3 Slow conduction and propagation failure through a tapered region of a synthetic strand of cardiac muscle at normal (upper) and rapid (lower) rates of stimulation. Records were obtained from cells within bulbous segments (A and D) and the intervening tapering region (B and C) at distances of 300 $\mu$m (A–B), 100 $\mu$m (B–C), and 500 $\mu$m (C–D). The extracellular stimulating electrode was positioned 5.0 mm from A and rates of stimulation are indicated by cycle lengths in frames A (upper and lower). Calibration pulse: 20 mV and 20 ms.

region of 0.02 m/s was thus largely the result of slow propagation in a localized region where the conduction velocity is an order of magnitude less.

Although proximal to the regions of block, action potentials propagate at normal velocity; their shape is influenced by the distal region of slow conduction and beyond. Action potentials recorded proximal to a region of 2:1 block showed alternate changes in shape. These changes in shape are clearly seen in Figs. 3 and 4 and are similar to those recently reported for isolated Purkinje fibers proximal to an area of intermittent block (3). Regions of the strand at distances of 0.9–1.6 mm proximal to the area of intermittent block appeared to be unaffected since the shapes of all action potentials were identical (Figs. 2, 3 A, 4 A). Interactions between regions

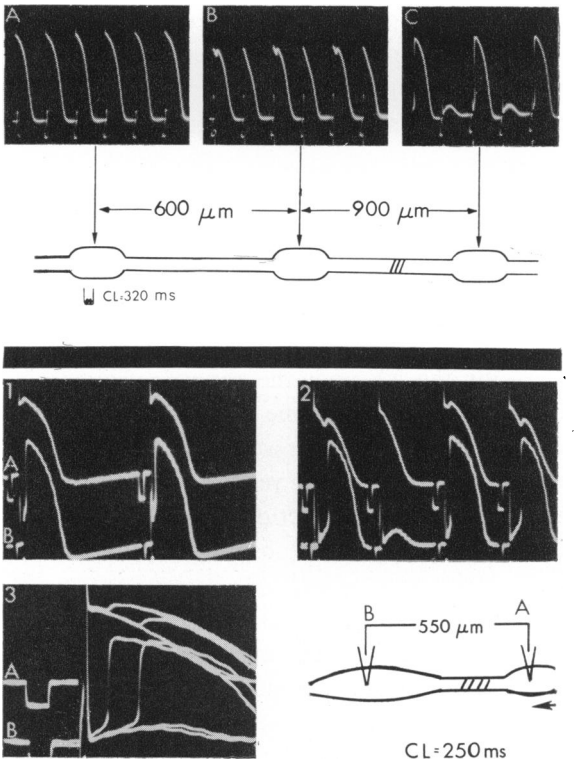


FIGURE 4 Relationship between conduction failure and action potential duration in a synthetic strand at high rates of stimulation. Upper panel: transmembrane action potentials obtained sequentially from the bulbous areas indicated. Position of the stimulating electrode is indicated to the left of the drawing. Lower panel: records obtained simultaneously from the positions indicated. Frame 3 is an expanded, superimposed recording of a 3:2 Wenckebach cycle. The relationship between the presence of notches on the plateau of the proximally recorded action potental and successful distal propagation is evident. The arrow in the lower drawing points to the direction of impulse propagation initiated by an extracellular stimulating electrode positioned 3.0 mm from the recording electrode (A). The hatched areas indicate the region in which desynchronization of contraction was observed. Calibration pulse (upper and lower panels): 20 mV and 20 ms.

proximal and distal to areas of slow propagation are nicely demonstrated by the inflections on the plateau phase of the action potential recorded proximal to a region exhibiting a 3:2 Wenckebach cycle (Fig. 4 B). Excitation of the distal tissue causes the proximal action potential to revert to its normal time-course, producing the inflection on its plateau phase. Similarly, retrograde transmission of an action potential into a region of delayed propagation from one beyond is clearly responsible for the fast upstroke seen in Fig. 3 C. If the proximal electrode is moved away from the region of block, interactions of the above kind disappear (Figs. 2, 3 A, 4 A).

### *The Model*

All the mechanisms that have been suggested for decreases in conduction velocity can be divided into three groups, those involving changes in (*a*) geometry, (*b*) membrane properties, and (*c*) intercellular connections. Let us consider these possibilities one at a time, searching for a mechanism that could account for the low conduction velocity of 0.002 m/s that was described above for the synthetic strand.

*Geometry.* Discussions of mechanisms for slow conduction in cardiac muscle invariably postulate changes in geometry, no doubt prompted by light microscopic observations of the structure of the AV nodal region (9, 10). The mechanisms that have involved geometry have included long circuitous pathways, a change in fiber diameter, and a tapering in the number of fibers in a bundle. The simple morphology of the synthetic strand (17) immediately excludes mechanisms based on circuitous pathways; in the AV node the absence of discontinuous propagation led Hoffman and Cranefield (7) to the same conclusion.

Conduction velocity in a uniform fiber varies approximately as the square root of the fiber diameter (33, 34), and we have verified this relationship in our theoretical model as can be seen in Fig. 5 A. A reduction in conduction velocity from approximately 0.5 to 0.002 m/s would require an absurd reduction in diameter from 10 $\mu$m to 1.6 Å.

A discontinuity, such as an abrupt increase in the diameter of a fiber, causes a delay in propagation, but the maximum delay is small (35, 36). It has also been suggested that slow propagation in the AV node is due to frequent branching, resulting in an increase in the number of fibers in the direction of propagation (11). In our theoretical model, a 128-fold increase in the number of cell columns within 0.5 mm length produced a decrease in velocity of only 0.2%. Since this rate of branching is well beyond that realistically possible, considering the diameter of a cell, a change in velocity produced by branching can be discounted. This theoretical result is supported by our observation that in some synthetic strands (Fig. 1 A) where the overall diameter of the bundle decreased markedly and increased again, no change in velocity of propagation was detected. Ironically, then, geometry (7–11) cannot account for a conduction velocity as low as that found in the synthetic strand, AV node (1, 2), and embryonic AV ring (32).

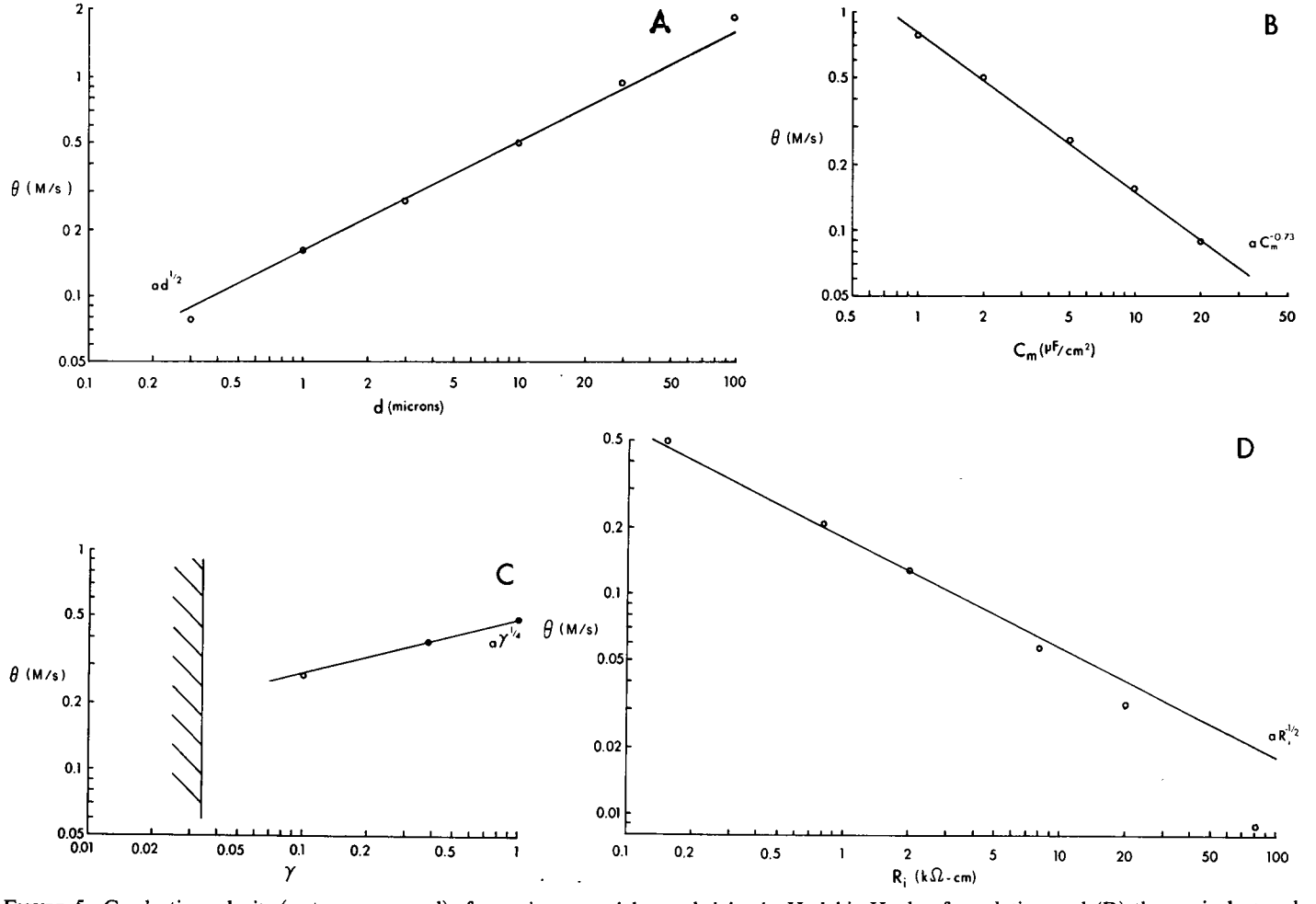


FIGURE 5 Conduction velocity (meters per second) of an action potential in the theoretical model as a function of (A) cell diameter $d$, (B) specific membrane capacitance $C_m$, (C) $\gamma$, the factor by which $g_K$ and $\bar{g}_{Na}$ were scaled in the Hodgkin-Huxley formulation and (D) the equivalent volume resistivity of the cytoplasm $R_i$. Hatching indicates the region of propagation failure.

*Membrane Properties*: $C_m$, $R_m$. Hodgkin (33) and Pickard (34) have pointed out that the conduction velocity down a uniform fiber should vary as $C_m^{-1/2}$ and we have confirmed this prediction (Fig. 5 B). Without seeking a purely theoretical upper limit for $C_m$ there are reasonable physicochemical grounds for limiting $C_m$ to more than 0.5 $\mu$F/cm$^2$ and less than 2 $\mu$F/cm$^2$, and known morphological grounds for keeping the effective $C_m$ below $\sim$20 $\mu$F/cm$^2$. As a result, this parameter could only account for about a sixfold decrease in $\theta$.

There are two basic ways of changing the specific membrane resistance $R_m$ in terms of the modified Hodgkin-Huxley formulation used here. One is to directly alter the kinetics of change of the sodium conductance $g_{Na}$ and the other is to alter the values of the maximum sodium conductance $g_{Na}$ and the steady potassium conductance $g_K$. To use the first method requires setting up arbitrary modifications of the Hodgkin-Huxley formulation or entirely new systems, a speculation which would seem to us unprofitable, without the constraint of more experimental facts. The second method, in effect, changes the number of active sites per unit area of membrane, leaving the voltage-dependent kinetics of each site unchanged. Paes de Carvalho et al. (13) have in effect suggested an extreme example of this, postulating that the slow rate of depolarization and conduction in the cells of the AV node is due to the absence of a fast sodium-carrying mechanism of the Hodgkin-Huxley type. A similar supposition for slow conduction in the synthetic strands would be to say that cells are connected by fibroblasts (37, 38) that presumably lack such a mechanism. Pickard (34) showed that the conduction velocity should vary as the maximum rate of rise of the sodium conductance raised to the one-fourth power. We found that if $g_{Na}$ and $g_K$ were scaled down together, the conduction velocity varied as the fourth root of the scaling factor down to the point where propagation ceased (Fig. 5 C). Reducing the conductances by a factor of $\frac{1}{10}$ reduced the conduction velocity to 54%. When the factor was decreased to $\frac{1}{30}$, in an attempt to reduce the conduction velocity further, propagation failed.

The question arises: can one achieve an *effective* slow conduction velocity by causing a local delay, relinquishing the constraint that uniform propagation be maintained? The extreme example of this case would be the coupling of two normal areas of membrane with purely passive membrane that is devoid of nonlinear properties. This case was simulated by the following model. The two active areas of membrane were simulated by two patches[3] of Hodgkin-Huxley membrane (modified as in Methods) and these were coupled by a passive cable described by the following parameters:

$R_m = 10^8$ Ω-cm$^2$,
$R_i = 150$ Ω-cm,

[3] Since, in this case, we were interested only in the delay produced by the passive cable, the effects of propagation in the active regions were neglected in order to simplify the model and shorten the computations.

$C_m$ = 2 $\mu$F/cm$^2$,
diameter $d$ = 3 $\mu$m,
length $l$ = 0.13 mm.

This set of parameters was chosen to maximize the delay as follows. The specific membrane resistance $R_m$ was made very high to allow all the current entering the passive cable to leave it on the other side. The intracellular resistivity $R_i$ was set equal to that estimated for cardiac muscle (39). The specific membrane capacitance, $C_m$ was 2 $\mu$F/cm$^2$, a reasonable maximum value for the reasons given above. The value of 3 $\mu$m for the diameter was based on electron micrographic observations of the synthetic strand (22).

The passive cable was made as long as possible, consistent with successful excitation of the distal active patch. Assuming no current loss through the passive membrane, this length can be shown to be

$$l = (K - 1) \frac{R_{mp}}{R_i} \frac{\pi d^2}{4A_p}, \qquad (7)$$

where $K$ is the ratio of action potential amplitude to threshold potential (measured with respect to resting potential), $R_{mp}$ is the specific membrane resistance of the distal active patch, and $A_p$ is the area of the patch. $K$ was chosen to be 10 and $A_p$ 0.001 cm$^2$ (see below) and $R_{mp}$ was set as high as would allow a stable resting potential (2.8 k$\Omega$-cm$^2$).

With these parameter values, the total delay between the two patches was 10.6 ms (Fig. 6). Most of the delay occurs not in propagation down the passive cable but in the slow turn-on of the distal active patch. Since the membrane resistance of the active patch is small compared with the longitudinal coupling resistance, the turn-on is governed by the resting membrane time constant of the active patch $R_{mp}C_m$ which was 5.6 ms. The contribution of the delay in the passive cable to the total delay can become significant only when preposterous values for $A_p$ and $l$ are assumed. If $A_p$ is assumed to be as small as the area of one cell ($\sim 10^{-5}$ cm$^2$), $K$ must also be reduced to about 3, since charging of the capacitance of the cable will be completed not during the spike but during the plateau. The resulting value for $l$ in Eq. 7 is 2.9 mm, which would give a delay of $\sim$6.0 ms. Since the delay in the passive cable is proportional to $R_iC_m/d$, reasonable values of $C_m$ ensure that the membrane properties of the passive cable play little or no role in the delay. It would seem therefore that coupling by a cell with inactive membrane and/or high $C_m$ could not account for slow conduction. In fact, the dominating factor in the delay is the magnitude of the coupling resistance, which in this case is the longitudinal resistance of the coupling cable. We will take up the case of intercellular coupling by a high resistance in the next section.

*Intercellular Connections.* The question arises: how do junctional properties affect conduction velocity? As a partial answer to this question, we have ex-

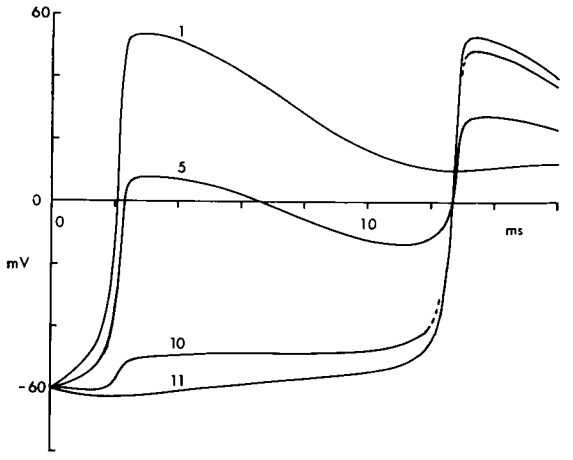


FIGURE 6 Wave forms of action potentials from model of two active patches interconnected by a passive cable. Traces 1 and 11 are from the proximal and distal active patches, respectively. Traces 5 and 10 are from a central and the distal segment of the passive cable.

amined the effects of increases in a purely linear coupling resistance. Initially, we studied the extreme case of two excitable cables coupled by a single high resistance junction. This is a model similar to that used by Heppner and Plonsey (40) to study the limits imposed on the coupling resistance by the requirement of successful transmission between two cells.

As in the case of our two patch-passive cable model, we found that there was an upper limit to the value of the coupling resistance, which in this case was about six times the resting input resistance of the distal cable. The magnitude of the delay as a function of the coupling resistance is shown in Fig. 7. Avoiding the just-threshold region in the distal cable, the maximum propagation delay across a single resistive junction was found to be around 6.0 ms (specific membrane capacitance 2 $\mu F/cm^2$).

If the distal input resistance of the cell column was increased, the coupling resistance could be increased by a similar factor, producing more delay. In our generalized cable model each element represents a length $\Delta x$, of a uniform, one-dimensional cable, where $r_i$ represents the cytoplasmic resistance. Pickard (34) predicted that the conduction velocity should vary as $R_i^{-1/2}$ and this we confirmed (Fig. 5 D). When the cable is continuous, $r_i$ can be increased without limit, producing any arbitrarily slow velocity of propagation. When the cable is segmented, however, as it must be for numerical solution, for a given $\Delta x$ there is a limit to $r_i$ above which propagation ceases and the model fails to represent a continuous cable. Normally, this would call for a reduction in $\Delta x$, but if $\Delta x$ is thought of as representing the length of a single cell, and $r_i$ as the resistance of intercellular connections rather than that of the cytoplasm, then $\Delta x$ cannot be reduced below a reasonable cell length. For our value of $\Delta x$ (60 $\mu$m), the limit for $r_i$ is somewhat above 500 times normal.

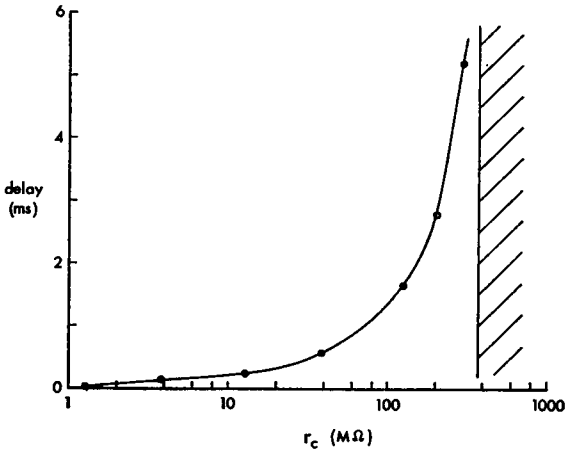


FIGURE 7 Delay in conduction between two uniform active cables ($d$ = 3 μm, $C_m$ = 2 μF/cm²) as a function of the resistance $r_c$ coupling them. Hatching indicates the region of propagation failure.

In other words, the resistors $r_i$ represent the combined resistance of the cytoplasm and the cell junctions, so that large values of $r_i$, in essence, solely represent the resistance of a junctional complex. For simplicity in the model, the resistance to longitudinal current was assumed to be entirely intracellular. Effects identical with those produced by an increase in $r_i$ would also be produced by an increase in extracellular resistance provided that the extracellular current was also restricted to one dimension. This might occur if extracellular space was constricted to a thin annulus around the cell column. Such an annulus, were it of salt solution (volume resistivity equals 50 Ω-cm) would be only 100 Å thick in order for the extracellular resistance per unit length to equal 500 times the normal $r_i$.

Since slowly conducting tissue eventually must couple back to normal fast conducting tissue, the coupling resistance between successive cells must be reduced gradually. We studied a nonuniform cable where $r_i$ was increased gradually from element to element to a value 500 times normal for two values of $r_i$ and then decreased gradually back to normal. The overall delay for this case was 41.3 ms. If more delay is desired, the central region, where $r_i$ is at its maximum value, can be widened to more than two elements. For example, an overall delay of 100 ms for the cable with tapered properties could be obtained by extending the central section to a length of 0.53 mm, giving an overall length of the preparation of 1.7 mm, not an unreasonable path length for an AV node with a delay of 100 ms.

This model, however, still cannot account for the conduction velocity of 0.002 m/s that was observed in the synthetic strand. A reduction of the cell diameter from 10 μm to a minimum compatible with histological findings (3 μm) would further slow conduction only 33%. The additional slowing requires one further assumption, namely, a change in membrane properties concomitant with the progressive change

in $r_i$. We reduced simultaneously $g_{Na}$ and $g_K$ in the modified Hodgkin-Huxley formulation which could be thought of as a gradual reduction in the number of channels in the membrane per square centimeter. This assumption has a dual effect: it reduces the excitatory current and causes a reduction in the rate of depolarization, but what is more important, the reduction in resting membrane conductance allows the coupling resistance between cells to be increased further. We reduced the Hodgkin-Huxley conductances by a factor of one-fourth in the center (tapering linearly from unity at the ends) and increased $r_i$ by an additional factor of four to a maximum value of 2000 times normal in the center. This resulted in an overall conduction delay for the 1.2 mm cable of 460 ms (vs. 41.3 ms for the previous case). The slowest conduction velocity achieved in the central regions was approximately 0.0005 m/s. These values were more than adequate to account for those observed in the synthetic strand.

## DISCUSSION

Slow conduction in cardiac muscle has been attributed to "decremental conduction", a term used to describe a progressive (graded) diminution in the amplitude and rate of depolarization of the action potential with distance (1). Although this phenomenon is invariably associated with slowing conduction, it is by no means clear that there is a *causal* relationship. The considerable attention that has been given to the cause of decremental conduction no doubt stems from this implied relationship. Progressive increase in threshold, fiber diameter, increasing membrane capacitance, membrane resistance, and low resting potential have all been implicated in speculations as to the cause of decremental conduction (1). The proponents of decremental conduction also propose as an additional cause of slow conduction, "very slow conduction," a phenomenon of equally obscure mechanism (3). Whether either of these can account for slow conduction is now an irrelevant question; our findings show that none of the factors said to underlie them could reasonably account for a slowing of conduction of the magnitude considered here.

Previous authors have related a decrease in conduction velocity to an increase in $R_i$ (16, 41) and others have attempted to relate the extent and distribution of nexuses or gap junctions to slow conduction and/or the degree of electrical coupling between cells (9, 10, 14, 15, 42). It would appear, however, that the nexus is not the only structural correlate of resistive coupling between cells. There are no such forms of close cell apposition in frog atrial and ventricular muscle (43), yet resting and action potentials have been recorded from frog atrial trabeculae and muscle strips using the double sucrose gap (44, 45). In regions of slow conduction in the synthetic strand, although the number of cells is invariably small, the junctional complexes between them are indistinguishable from those observed in rapidly conducting regions elsewhere (22). In our view, the conclusion to be drawn from this finding and those in the present paper is that morphological specialization of junctional com-

plexes develops independently of electrophysiological specializations, which in this case would be the development of intercellular resistive channels through one or more of the components of a junctional complex.

Notches or abrupt changes in potential were seen during repolarization near regions of slow propagation in the synthetic strand and have been seen in other preparations of cardiac muscle (3, 4, 6, 7, 11, 15). We made no attempt to interpret these notches through the theoretical model since their simulation depends on a proper description of repolarization in the model; the input current-voltage relationship during the repolarization phase determines the character and degree of electrical coupling between regions and hence the form of these and other interactions.

Slow conduction is a necessary condition for reentry, a phenomenon which is said to be the fundamental mechanism underlying cardiac arrhythmias (3, 46). The necessary conditions for slow conduction that we have shown to be the most reasonable could no doubt be produced by tissue damage (infarct), anoxia, and localized exposure to high $K$, but it is difficult to see how these conditions could be produced by an appropriately timed electrical stimulus to normal tissue, an intervention known to initiate all kinds of arrhythmias. It would seem to us that perhaps another mechanism (e.g., repetitive firing [47]) would be a more appropriate explanation for these arrhythmias.

*Note Added in Proof.* Our attention has been drawn to an addendum to a paper by Cranefield et al. (1972, *J. Gen. Physiol.* **59**:227) in which the authors refer to an early communication of ours (1971, *J. Gen. Physiol.* **58**:711, abstract) that describes the phenomenon of slow conduction in the synthetic strand. In their addendum, the authors have apparently gained the impression from our communication that the slow conduction we described was the result of a narrowing of the strand to a few fibers. It was not our intention to create such an impression and we hope the present paper has demonstrated, unequivocally, that it is a misconception.

The authors wish to thank Ms. Anne E. Roggeveen for her excellent management of the tissue culture preparations.
The technical assistance of Mr. Owen W. Oakeley and Ms. Estell Clark is greatly appreciated.

This research was supported in part by grants from the National Institutes of Health (HL 12157 and HL 43004), North Carolina Heart Association, and an Established Investigatorship from the American Heart Association (71160) to Dr. Lieberman.

*Received for publication 21 February 1972 and in revised form 8 May 1972.*

## REFERENCES

1. HOFFMAN, B. F., A. PAES DE CARVALHO, W. C. MELLO, and P. F. CRANEFIELD. 1959. *Circ. Res.* **7**:11.
2. SPACH, M. S., M. LIEBERMAN, J. G. SCOTT, R. C. BARR, E. A. JOHNSON, and J. M. KOOTSEY. 1971. *Circ. Res.* **29**:156.
3. CRANEFIELD, P. F., H. O. KLEIN, and B. F. HOFFMAN. 1971. *Circ. Res.* **28**:199.
4. WENNEMARK, J. R., V. J. RUESTA, and D. A. BRODY. 1968. *Circ. Res.* **23**:753.
5. ALANIS, J., D. BENITEZ, and G. PILAR. 1961. *Acta Physiol. Latinoamer.* **11**:171.
6. MENDEZ, C., W. J. MUELLER, and X. URGUIAGA. 1970. *Circ. Res.* **26**:135.

7. HOFFMAN, B. F., and P. F. CRANEFIELD. 1960. Electrophysiology of the Heart. McGraw-Hill Book Company, New York.
8. SANO, T., F. SUZUKI, and S. TAKIGAWA. 1964. *Jap. J. Physiol.* **14**:659.
9. JAMES, T. N., and L. SHERF. 1968. *Circulation.* **37**:1049.
10. DEFELICE, L. J., and C. E. CHALLICE. 1969. *Circ. Res.* **24**:457.
11. KANNO, T. 1970. *Jap. J. Physiol.* **20**:417.
12. MERIDETH, J., C. MENDEZ, W. J. MUELLER, and G. K. MOE. 1968. *Circ. Res.* **23**:69.
13. PAES DE CARVALHO, A., B. F. HOFFMAN, and M. DE PAULA CARVALHO. 1969. *J. Gen. Physiol.* **54**:607.
14. DEWEY, M. M., and L. BARR. 1964. *J. Cell Biol.* **23**:553.
15. MARTINEZ-PALOMO, A., J. ALANIS, and D. BENITEZ. 1970. *J. Cell Biol.* **47**:1.
16. SPERELAKIS, N., G. MAYER, and R. MACDONALD. 1970. *Am. J. Physiol.* **219**:952.
17. LIEBERMAN, M., A. E. ROGGEVEEN, J. E. PURDY, and E. A. JOHNSON, 1972. *Science* (*Wash. D. C.*). **175**:909.
18. LIEBERMAN, M. 1967. *Circ. Res.* **21**:879.
19. VUREK, G. G., C. M. BENNETT, R. L. JAMISON, and J. L. TROY, 1967. *J. Appl. Physiol.* **22**:191.
20. KOOTSEY, J. M., and E. A. JOHNSON. 1972. *IEEE* (*Inst. Electr. Electron Eng.*) *Trans. Bio.-Med. Eng.* In press.
21. GAY, W. A., and E. A. JOHNSON. 1967. *Circ. Res.* **21**:33.
22. PURDY, J. P. 1971. The ultrastructure of growth oriented heart cells in tissue culture. M.S. Thesis. Duke University, Durham, North Carolina.
23. KATZ, B. 1939. Electric Excitation of Nerve. The Oxford University Press, London.
24. HODGKIN, A. L., and A. F. HUXLEY. 1952. *J. Physiol.* (*Lond.*). **117**:500.
25. WEIDMANN, S. 1955. *J. Physiol.* (*Lond.*). **127**:213.
26. NOBLE, D. 1962. *J. Physiol.* (*Lond.*). **160**:317.
27. JOHNSON, E. A., and M. LIEBERMAN. 1971. *Annu. Rev. Physiol.* **33**:479.
28. FITZHUGH, R. 1960. *J. Gen. Physiol.* **43**:867.
29. GEORGE, E. P., and E. A. JOHNSON. 1961. *Aust. J. Exp. Biol.* **39**:275.
30. MITCHELL, A. R., 1969. Computational Methods in Partial Differential Equations. John Wiley & Sons, Inc., London.
31. GERALD, C. F. 1970. Applied Numerical Analysis. Addison-Wesley Publishing Co., Inc., Reading, Mass.
32. LIEBERMAN, M., and A. PAES DE CARVALHO. 1965. *J. Gen. Physiol.* **49**:365.
33. HODGKIN, A. L. 1954. *J. Physiol.* (*Lond.*). **125**:221.
34. PICKARD, W. F. 1966. *J. Theor. Biol.* **11**:30.
35. KHODOROV, B. I., YE. N. TIMIN, S. YA. VILENKIN, and F. B. GUL'KO. 1969. *Biophysics.* **14**:323.
36. MARKIN, V. S., and V. F. PASTUSHENKO. 1969. *Biophysics.* **41**:336.
37. HYDE, A., B. BLONDEL, A. MATTER, J. P. CHENEVAL, B. FILLOUX, and L. GIRARDIER. 1969. *Prog. Brain Res.* **31**:283.
38. GOSHIMA, K. 1969. *Exp. Cell Res.* **58**:420.
39. WEIDMANN, S. 1952. *J. Physiol.* (*Lond.*). **118**:348.
40. HEPPNER, D. B., and R. PLONSEY. 1970. *Biophys. J.* **10**:1057.
41. HAUSWIRTH, O. 1969. *Circ. Res.* **24**:745.
42. BARR, L., M. M. DEWEY, and W. BERGER. 1965. *J. Gen. Physiol.* **48**:797.
43. BALDWIN, K. M. 1970. *J. Cell Biol.* **46**:455.
44. ROUGIER, O., G. VASSORT, and R. STÄMPFLI. 1968. *Pflügers Arch. Eur. J. Physiol.* **301**:91.
45. BROWN, H. F., and S. J. NOBLE. 1969. *J. Physiol.* (*Lond*). **204**:717.
46. CRANEFIELD, P. F., and B. F. HOFFMAN. 1971. *Circ. Res.* **28**:220.
47. MOE, G. K., A. S. HARRIS, and C. J. WIGGERS. 1941. *Am. J. Physiol.* **134**:473.
48. PLONSEY, R. 1969. Bioelectric Phenomena. McGraw-Hill Book Company, New York.

## APPENDIX

The derivation of the one-dimensional cable equation for an inhomogeneous cable (where $r_i$ is a function of $x$) follows closely the derivation of the classical cable equation (compare,

for example, Plonsey, 48). By Ohm's law, the variation in the potential in the axial direction must obey the equation.

$$\frac{\partial V}{\partial x} = -i_a r_i, \tag{A 1}$$

where $i_a$ is the axial current. Regardless of the detailed nature of the membrane current, conservation of charge requires that

$$\frac{\partial i_a}{\partial x} = -i_m. \tag{A 2}$$

Differentiating Eq. A 1 with respect to $x$,

$$\frac{\partial^2 V}{\partial x^2} = -i_a \frac{\partial r_i}{\partial x} - r_i \frac{\partial i_a}{\partial x}. \tag{A 3}$$

Note the extra term which appears since $r_i$ is not constant. Substituting from Eqs. A 1 and A 2 into Eq. A 3,

$$\frac{\partial^2 V}{\partial x^2} = \frac{1}{r_i} \frac{\partial r_i}{\partial x} \frac{\partial V}{\partial x} + r_i i_m, \tag{A 4}$$

which is equivalent to Eq. 2.